

# Roquin binds inducible costimulator mRNA and effectors of mRNA decay to induce microRNA-independent post-transcriptional repression

Elke Glasmacher<sup>1</sup>, Kai P Hoefig<sup>1,3</sup>, Katharina U Vogel<sup>1,3</sup>, Nicola Rath<sup>1</sup>, Lirui Du<sup>1</sup>, Christine Wolf<sup>1</sup>, Elisabeth Kremmer<sup>1</sup>, Xiaozhong Wang<sup>2</sup> & Vigo Heissmeyer<sup>1</sup>

The molecular mechanism by which roquin controls the expression of inducible costimulator (ICOS) to prevent autoimmunity remains unsolved. Here we show that in helper T cells, roquin localized to processing (P) bodies and downregulated ICOS expression. The repression was dependent on the RNA helicase Rck, and roquin interacted with Rck and the enhancer of decapping Edc4, which act together in mRNA decapping. Sequences in roquin that confer P-body localization were essential for roquin-mediated ICOS repression. However, this process did not require microRNAs or the RNA-induced silencing complex (RISC). Instead, roquin bound *ICOS* mRNA directly, showing an intrinsic preference for a previously unrecognized sequence in the 3' untranslated region (3' UTR). Our results support a model in which roquin controls ICOS expression through binding to the 3' UTR of *ICOS* mRNA and by interacting with proteins that confer post-transcriptional repression.

Roquin is a CCCH-type zinc finger protein that destabilizes the mRNA of the inducible costimulator (ICOS) in a process that requires the 3' untranslated region (3' UTR) of *ICOS* mRNA<sup>1</sup>. Loss of this post-transcriptional regulation causes autoimmunity in *Rc3h1<sup>san/san</sup>* mice, which are homozygous for a point mutation in *Rc3h1*, the gene that encodes roquin<sup>1,2</sup>. How *ICOS* mRNA is recognized by roquin protein and how this recognition induces mRNA decay is unknown at present.

Post-transcriptional regulation of gene expression controls key 'decisions' of innate and adaptive immune responses<sup>3–5</sup>. Pathways involved in translational repression and mRNA decay use many different molecular mechanisms but uniformly depend on *trans*-acting factors that bind to *cis*-regulatory elements in target mRNAs. One class of *trans*-acting factors are microRNAs (miRNAs) that, when loaded onto the RNA-induced silencing complex (RISC), can base pair with partially complementary sequences in the 3' UTR of target mRNAs<sup>5</sup>. RNA-binding proteins represent another class of *trans*-acting factors. *Cis* elements for these factors have been described in single-stranded RNA; however, they are not well defined and the recognition is thought to depend on shape as well as sequence<sup>3,6</sup>. *Trans*-acting RNA-binding proteins and miRNAs can target the same mRNA. The different *trans*-acting factors can cooperatively repress the target<sup>7</sup> or the RNA-binding protein can block miRNA-dependent repression<sup>8</sup>. In addition, *trans*-acting protein factors act together with miRNAs and central components of the RISC, the argonaute (Ago) proteins, in an opposing program and augment translation<sup>9</sup>. Whether the various pathways of post-transcriptional

regulation act together in general or work in parallel and converge under specific cellular conditions needs further investigation and requires genetic delineation of the molecules involved.

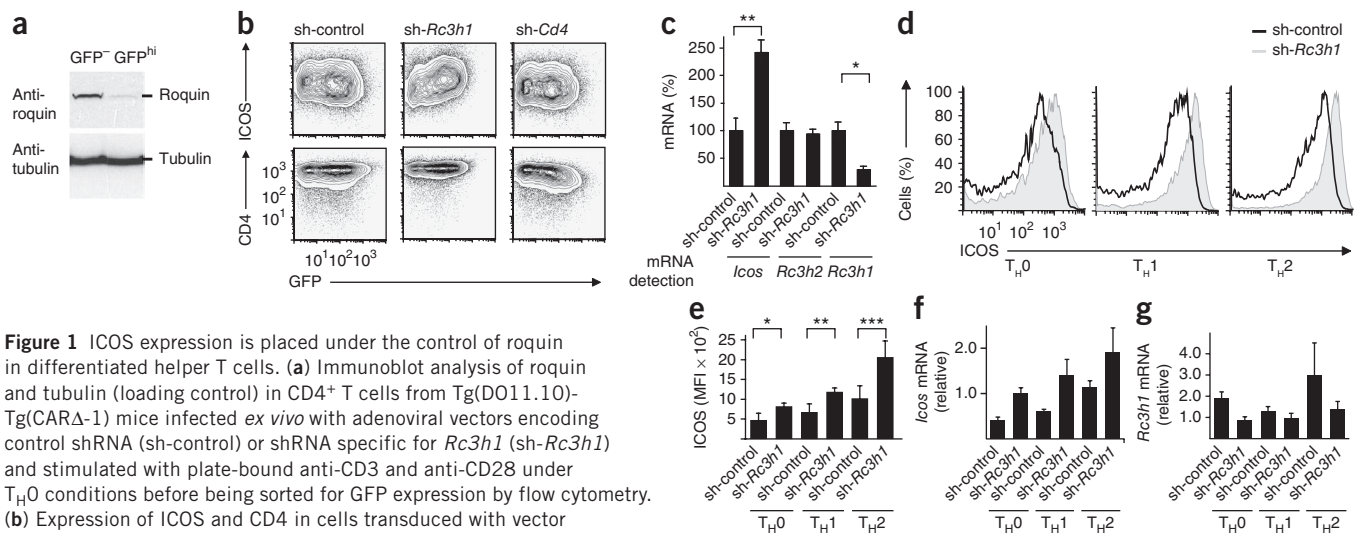
A 3' UTR region of *ICOS* mRNA has been described as being important for roquin-mediated repression of ICOS<sup>1</sup>. On the basis of the investigation of a putative miR-101-binding site in this region, functional dependence of roquin on miRNA has been suggested<sup>1</sup>. However, it remains unclear whether the miRNA itself or a roquin-miRNA or roquin-miRNA-induced silencing complex (miRISC) complex is the *trans*-acting factor that enables recognition of the mRNA and repression of cellular ICOS.

ICOS expression is substantially induced on the surface of T cells after recognition of antigen. Its transcription is upregulated early after triggering of the T cell antigen receptor and in response to activation of the transcription factor NFAT. However, the largest amounts of ICOS protein appear with a temporal delay, which demonstrates pronounced post-transcriptional regulation<sup>10</sup>. The induced ICOS expression regulates cytokine production in T cells, which allows them to provide B cells help for the production of high-affinity antibodies in the germinal center reaction<sup>11–15</sup>.

*Rc3h1<sup>san/san</sup>* mice that express mutant roquin proteins show spontaneous germinal center formation and develop autoimmune phenotypes similar to systemic lupus erythematosus in human patients<sup>2</sup>. Consistent with their aberrant high ICOS expression in T cells, these mice have more follicular helper T cells<sup>1,2,16</sup>. However, several autoimmunity-associated phenotypes disappear in *Rc3h1<sup>san/san</sup>* mice

<sup>1</sup>Helmholtz Zentrum München, German Research Center for Environmental Health, Institute of Molecular Immunology, Munich, Germany. <sup>2</sup>Department of Biochemistry, Molecular Biology and Cell Biology, Northwestern University, Evanston, Illinois, USA. <sup>3</sup>These authors contributed equally to this work. Correspondence should be addressed to V.H. (vigo.heissmeyer@helmholtz-muenchen.de).

Received 16 April; accepted 14 June; published online 18 July 2010; doi:10.1038/ni.1902



heterozygous for *Icos* deficiency<sup>1</sup>, which indicates that ICOS is the critical target in roquin-mediated prevention of lupus-like autoimmunity. The *Rc3h1*<sup>san/san</sup> mutation is positioned in the ROQ domain of roquin and renders it less effective in controlling ICOS expression<sup>1</sup>. The integrity of the ROQ domain is therefore essential in the prevention of autoimmunity; however, the molecular function of this domain remains unclear. Here we show that roquin is the *trans*-acting factor that targets *ICOS* mRNA for post-transcriptional repression. Roquin bound RNA through its ROQ domain and CCCH-type zinc finger and recognized a region in the 3' UTR of *ICOS*. Roquin also interacted with processing (P)-body factors, which are involved in mRNA decay, and was able to repress ICOS even in the complete absence of cellular miRNAs or RISC formation.

## RESULTS

### ICOS expression is controlled by roquin

To investigate the contribution of roquin to ICOS regulation in differentiated helper T cells, we established an adenoviral knock-down approach. We used primary CD4<sup>+</sup> T cells from Tg(DO11.10)-Tg(CARΔ-1) mice to introduce adenoviral vectors<sup>17</sup>. T cells from these mice are permissive for adenoviral infection through transgenic expression of a signaling-inactive version of the human coxsackie adenovirus receptor. We infected CD4<sup>+</sup> T cells before activating them with antibody to CD3 (anti-CD3) and anti-CD28 in culture conditions that skew helper T cell differentiation (Fig. 1). By using adenoviral vectors coexpressing green fluorescent protein (GFP) with short hairpin RNA (shRNA) specific for *Rc3h1* or the control gene *Cd4*, we were able to downregulate the expression of roquin protein (Fig. 1a) and *Rc3h1* mRNA (Fig. 1c,g). However, we observed downregulation of roquin protein only in cells with the highest expression of GFP (10–25%), which correlated with the observed lower efficiency of RNA-mediated interference in primary CD4<sup>+</sup> T cells<sup>18</sup>. Knockdown of roquin resulted in more ICOS protein and *Icos* mRNA in T helper

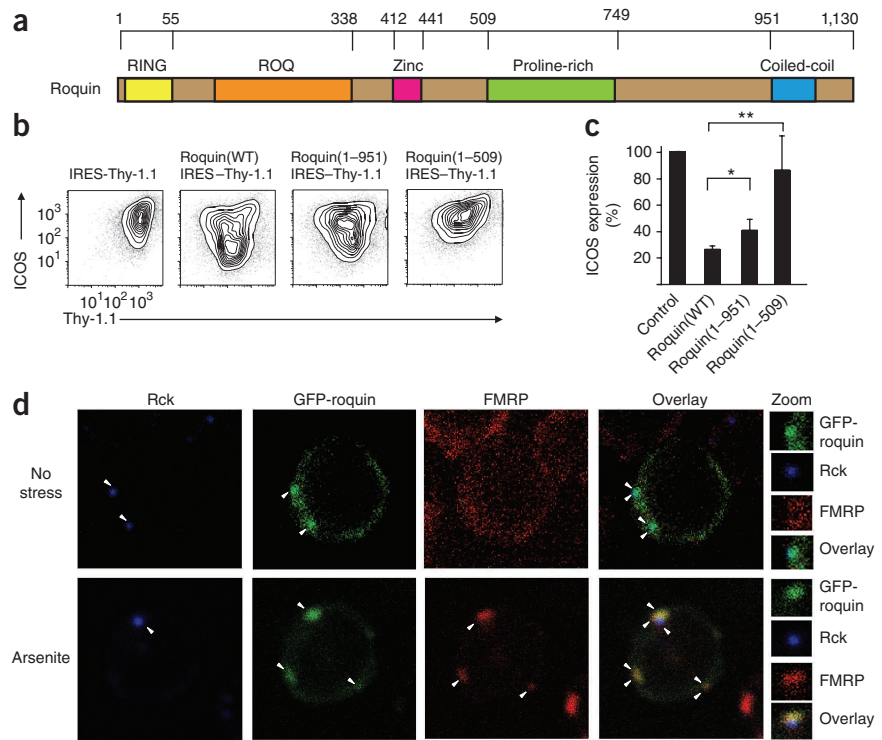
type 0 (T<sub>H0</sub>), T<sub>H1</sub> and T<sub>H2</sub> cells (Fig. 1b–f). The effect was specific, as it did not affect the expression of CD4 protein (Fig. 1b) or *Rc3h2* mRNA (Fig. 1c), the paralog of *Rc3h1* (ref. 19). In addition, ICOS expression was not induced by expression of an empty shRNA vector or by knockdown of CD4 (Fig. 1b). Quantification of the surface expression of ICOS protein (Fig. 1d,e) and *Icos* mRNA (Fig. 1f) during the activation and differentiation of CD4<sup>+</sup> T cells under T<sub>H0</sub>, T<sub>H1</sub> and T<sub>H2</sub> conditions demonstrated that ICOS protein and *Icos* mRNA increased from T<sub>H0</sub> cells to T<sub>H1</sub> cells to T<sub>H2</sub> cells (Fig. 1d–f), as reported before<sup>10</sup>. Regardless of the differentiation conditions, there was a significant increase in ICOS surface expression in cells transduced with shRNA specific for *Rc3h1* (Fig. 1d,e). We observed a similar increase in *Icos* mRNA in the bulk population containing 72–90% GFP<sup>+</sup> cells (Fig. 1f). The knockdown diminished *Rc3h1* mRNA to 46–75% of endogenous amounts in the bulk population (Fig. 1g). These findings show that the expression of ICOS is placed under the post-transcriptional control of roquin in helper T cells.

### Roquin interacts with the P-body pathway

We used deletion mutagenesis to identify regions in roquin critical for the repression described above. We analyzed the mutants in mouse embryonic fibroblasts (MEFs) first transduced with retrovirus expressing full-length human *ICOS* mRNA and subsequently superinfected with retrovirus containing an internal ribosomal entry site coexpressing the marker Thy-1.1 and wild-type or mutant versions of roquin. Truncation of the carboxyl terminus in mutant roquin(1–509), which consists of amino acids 1–509 and lacks the proline-rich and the coiled-coil regions, inactivated roquin-mediated repression of ICOS (Fig. 2a–c). In contrast, roquin(1–951), a mutant lacking only the carboxy-terminal coiled-coil domain, was slightly less active than wild-type roquin (Fig. 2a–c).

The inactive roquin(1–509) mutant fused to GFP showed aberrant diffuse cytoplasmic localization after transfection into HEK293 human

**Figure 2** Carboxy-terminal sequences in roquin are required for ICOS repression and roquin localization. **(a)** Domain organization of roquin, including the RING finger, ROQ domain, zinc finger, a region rich in proline, and the coiled-coil domain. Numbers above indicate amino acid positions used as amino- or carboxy-terminal ends of deletion mutants. **(b)** Expression of ICOS and roquin (assessed as Thy-1.1) in MEFs transduced with a retrovirus encoding full-length human ICOS mRNA and superinfected with a retrovirus containing an internal ribosomal entry site and Thy-1.1 (IRES-Thy-1.1) alone or with wild-type roquin (roquin(WT)) or mutant roquin (roquin(1–951)) or roquin(1–509). Data are representative of three experiments. **(c)** ICOS expression in the cells in **b**, presented relative to its expression in control cells (empty Thy-1.1 vector), set as 100%. \* $P = 0.027$  and \*\* $P = 0.008$  (one-way ANOVA). Data are from three independent experiments (average and s.d.). **(d)** Confocal microscopy of the colocalization of Rck (blue) and FMRP (red) with GFP-tagged wild-type roquin (GFP-roquin; green) in primary CD4<sup>+</sup> T cells with (Arsenite) and without (No stress) arsenite treatment after 48 h of stimulation with plate-bound anti-CD3 and anti-CD28. White arrowheads indicate Rck-, GFP- and FMRP-labeled foci. Zoom (far right), enlargement of images at left. Original magnification,  $\times 232$  (main images) or  $\times 262$  (far right). Data are representative of two experiments.



embryonic kidney cells (**Supplementary Fig. 1a**), in contrast to the localization of fusion proteins of GFP and roquin(1–951) or wild-type roquin, which localized to cytoplasmic foci and showed little diffuse cytoplasmic staining (**Supplementary Fig. 1a,b**). We assessed roquin localization in primary CD4<sup>+</sup> T cells transduced with adenoviruses expressing GFP–wild-type roquin (**Fig. 2d** and **Supplementary Fig. 1c**) and HEK293 cells transfected with GFP–wild-type roquin (**Supplementary Fig. 1b**) by costaining with antibodies that robustly identify P bodies or stress granules. Many of the roquin-enriched foci in HEK293 or CD4<sup>+</sup> T cells showed full colocalization with the RNA helicase Rck and we therefore identified them as P bodies<sup>20</sup>. In contrast, FMRP, a marker protein of stress granules<sup>21,22</sup>, showed diffuse staining in both cell types in the presence or absence of ectopic roquin expression (**Fig. 2d** and **Supplementary Fig. 1b**). Consistent with that, staining with an antibody to the stress granule marker G3BP1 confirmed the absence of stress granules in CD4<sup>+</sup> T cells after expression of roquin (**Supplementary Fig. 1c**). Quantification of localization of GFP-roquin fusion proteins in CD4<sup>+</sup> T cells showed that in 62% of the cells, roquin was associated with P bodies, whereas it localized to the stress granules in only 1.7% of the cells. There was no effect of roquin expression on the percentage of cells with P bodies (68% of all cells) or stress granules (18% of all cells) or on the number of P bodies or stress granules per cell (data not shown).

Subjecting CD4<sup>+</sup> T cells to arsenite-induced stress (**Fig. 2d**) induced the formation of stress granules in 85% of cells, and 89% of cells expressing GFP-roquin showed an association of roquin with stress granules. Roquin remained associated with P bodies in only 5.5% of these cells. Experimental induction of stress changed neither the percentage of cells positive for P bodies nor the number of P bodies per cell (on average, 2) or stress granules per cell (on average, 2.75; data not shown). Similarly, in HEK293 cells, the colocalization of roquin and Rck was nearly completely abrogated in cells treated with arsenite to

induce oxidative stress (**Supplementary Fig. 1b**). During aggregation of the messenger ribonucleoprotein complexes that form P bodies, sequences rich in glutamine and asparagine mediate protein–protein interactions<sup>23–25</sup>. The carboxy-terminal region of roquin showed a greater frequency of glutamine and asparagine residues in sequences adjacent to the proline-rich region<sup>25</sup>. Artificially defined frames of 80 amino acids reach a maximum content of 17 glutamine and asparagine residues in mouse roquin, with 7.68 as the predicted average<sup>25</sup>. We therefore investigated localization and function of the mutant roquin(1–749), which contains the proline-rich region but lacks the sequences enriched in glutamine and asparagine residues. This mutant had impaired foci formation in the absence of stress (**Fig. 3a**) but was still able to translocate into stress granules after arsenite treatment (**Fig. 3a**). Overexpression of this mutant interfered with P-body formation, as judged by the diffuse cytoplasmic localization of Rck (**Fig. 3a**). However, after the induction of stress, the Rck-labeled foci quickly reappeared (**Fig. 3a**). In functional assays, roquin(1–749) was considerably impaired in its ability to downregulate ICOS after sequential infection of the mouse fibroblast cell line NIH3T3 (**Fig. 3b,c**). These findings positively correlate roquin function with its localization to P bodies but not with its localization to stress granules.

To investigate the possibility that stress granules are dispensable, we tested roquin function in the absence of T cell intracellular antigen 1 (TIA-1; **Supplementary Fig. 2c**). TIA-1-deficient MEFs have impaired assembly of stress granules, as determined by staining for the stress granule markers TIAR, eIF3 and G3BP<sup>26</sup>. In TIA-1-deficient and control MEFs (**Fig. 3d**) sequentially transduced with retroviral ICOS and roquin constructs, there was almost no effect of *Tia1* deletion on the ability of roquin to repress ICOS (**Fig. 3d,e**). The data suggest that at least in the absence of cell stress, roquin-mediated repression of ICOS does not depend on TIA-1 function and instead requires physical or functional interactions with P-body components.

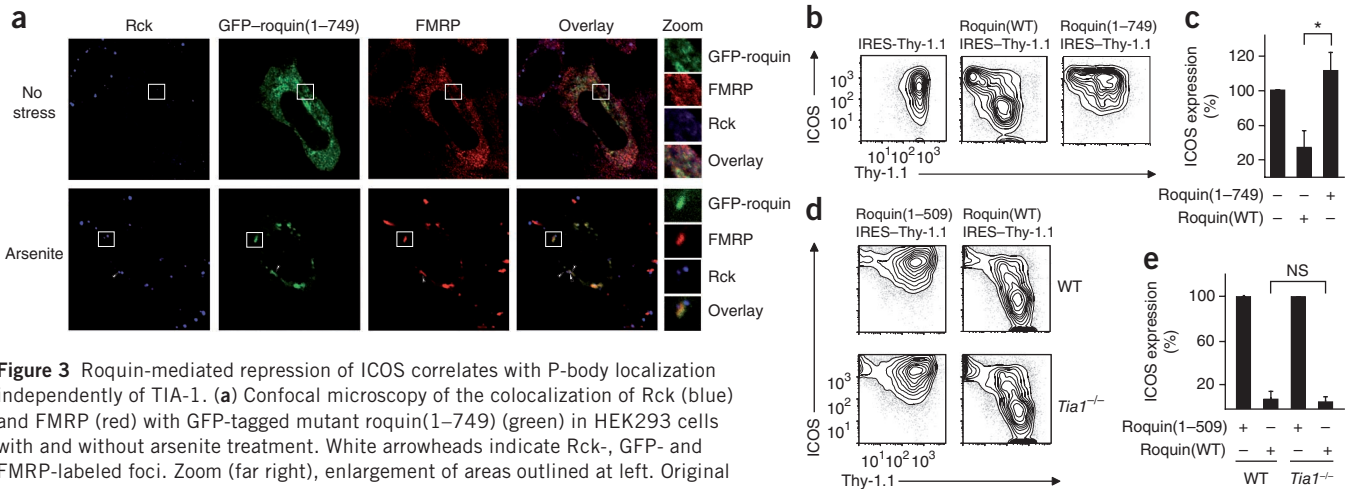


**Figure 3** Roquin-mediated repression of ICOS correlates with P-body localization independently of TIA-1. (a) Confocal microscopy of the colocalization of Rck (blue) and FMRP (red) with GFP-tagged mutant roquin(1-749) (green) in HEK293 cells with and without arsenite treatment. White arrowheads indicate Rck-, GFP- and FMRP-labeled foci. Zoom (far right), enlargement of areas outlined at left. Original magnification,  $\times 57$  (main images) or  $\times 104$  (far right). Data are representative of two experiments. (b-e) Expression of ICOS and roquin (assessed as Thy-1.1) in NIH3T3 cells (b,c) or wild-type and TIA-1-deficient MEFs (d,e) infected and assessed as described above (Fig. 2b,c). \* $P = 0.006$ , roquin(1-749) versus roquin(WT) (c); NS, not significant ( $P = 0.07$ ), TIA-1-deficient versus wild-type cells (e; one-way ANOVA). Data are representative of three independent experiments (error bars (c,e), average and s.d.).

### Roquin interacts with decapping proteins

To identify roquin-interacting proteins, we generated a rat monoclonal antibody directed against an internal peptide of roquin (Supplementary Fig. 2a,b). By mass spectrometry, we identified the helicase Rck (an essential component of the decapping pathway), the enhancer of decapping Edc4 and the decapping activator Dcp1a in extracts of  $T_H1$  cells immunoprecipitated with purified anti-roquin coupled to magnetic beads but not in control precipitations (beads coupled to an irrelevant antibody; data not shown). We confirmed by coimmunoprecipitation that Edc4 and Rck were associated with roquin protein in  $T_H1$  cells (Fig. 4a) and in MEFs (Fig. 4b). Edc4 interacted more strongly than did Rck, because the protein seemed enriched in immunoprecipitation relative to its presence in input. Rck was substantially and specifically associated with but was not enriched in anti-roquin immunoprecipitations compared with input amounts. GFP-tagged roquin(1-509) also interacted with endogenous Edc4 in anti-GFP immunoprecipitates from extracts of adenovirus-transduced MEFs (Fig. 4c). The interaction occurred through amino-terminal sequences in roquin, did not require localization of roquin to P bodies (Fig. 3a and Supplementary Fig. 1a) and was insensitive to RNase treatment during the immunoprecipitation procedure that efficiently degraded the 28S and 18S rRNA in RNA extracts prepared from immunoprecipitation supernatants (Fig. 4c and data not shown). Consistent with a possible association of all three proteins in one complex, we observed full colocalization of Edc4, Rck and GFP-roquin in HEK293 cells in the absence of stress induction (Supplementary Fig. 2d).

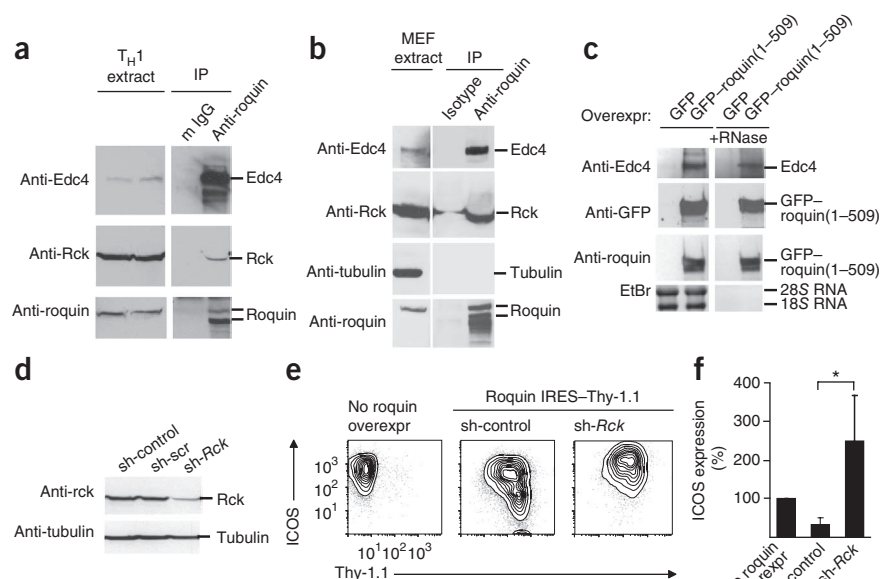
Experimentally lowered amounts of cellular Rck protein (Fig. 4d) in MEFs transduced with retrovirus encoding ICOS as well as retrovirus encoding roquin linked to internal ribosomal entry site-Thy-1.1 expression led to effective derepression of ICOS (Fig. 4e,f). We achieved knockdown by superinfection of retrovirally transduced MEFs with adenovirus encoding shRNA specific for the gene encoding Rck (*Ddx6* (called 'Rck' here); Fig. 4d), and ICOS expression was higher than before roquin transduction (Fig. 4e,f). This experiment indicated that knockdown of Rck neutralized the function of exogenous as well as endogenous roquin protein, which is detectable in MEFs (data not shown). These data are consistent with a model

in which roquin mediates silencing of ICOS through functional and physical interaction with proteins of the decapping pathway.

### Roquin-mediated repression does not require miRNA

Rck is not only required in the decapping pathway but is also essential in miRNA-dependent post-transcriptional silencing<sup>20</sup>. This pathway has been linked to roquin-mediated ICOS repression<sup>1</sup>. We generated MEF clones deficient in the endoribonuclease Dicer by transducing cells with two loxP-flanked alleles of *Dicer1* (*Dicer1<sup>fl/fl</sup>*), as well as wild-type cells, with retrovirus expressing Cre recombinase. In parallel, we used CD4<sup>+</sup> T cells from *Dicer1<sup>fl/fl</sup>* and *Dicer1<sup>+/fl</sup>* mice with Cre expression driven by *Cd4* regulatory elements. Real-time PCR analysis of several candidates and global high-throughput sequencing of small RNAs showed almost undetectable miRNA in Dicer-deficient MEF clones<sup>27</sup> (Supplementary Fig. 3a,b). In contrast, although peripheral CD4<sup>+</sup> T cells from *Dicer1<sup>fl/fl</sup>* mice with *Cd4* regulatory element-driven Cre expression showed efficient deletion of the targeted alleles (Supplementary Fig. 3c), detection of miRNA revealed more than 20% of residual endogenous expression of the miRNAs miR-101, miR-155 and miR-181 (Supplementary Fig. 3d). These findings suggested a very long half-life of RISC-loaded miRNAs during T cell development and, at the same time, ruled out the possibility of testing a requirement for miRNA in roquin-mediated ICOS expression in CD4<sup>+</sup> T cells. We therefore infected wild-type and Dicer-deficient MEFs with retrovirus encoding ICOS and wild-type roquin or ICOS and roquin(1-509) (Fig. 5a,b). Wild-type roquin, unlike its inactive mutant, efficiently downregulated surface expression of ICOS in wild-type and Dicer-deficient cells (Fig. 5a,b). Moreover, roquin-mediated repression of ICOS occurred in wild-type cells and in Dicer- and miRNA-deficient cells with a similar dose response, as shown by quantification of ICOS on cells with low, intermediate or high surface expression of Thy-1.1, the marker coexpressed by the roquin-encoding retrovirus (Fig. 5c). In addition, roquin induced a similar decrease of ICOS mRNA expression in wild-type and Dicer-deficient cells (Fig. 5d). Expression of wild-type roquin and roquin(1-509) was equal in wild-type and Dicer-deficient cells (Supplementary Fig. 3e, lane 1 versus lane 4, and lane 2 versus lane 3). We did not detect higher expression of endogenous roquin protein (Supplementary Fig. 3e, lanes 1 and 4, and f) or *Rc3h1* mRNA (data not shown) in cells with deletion of Dicer.

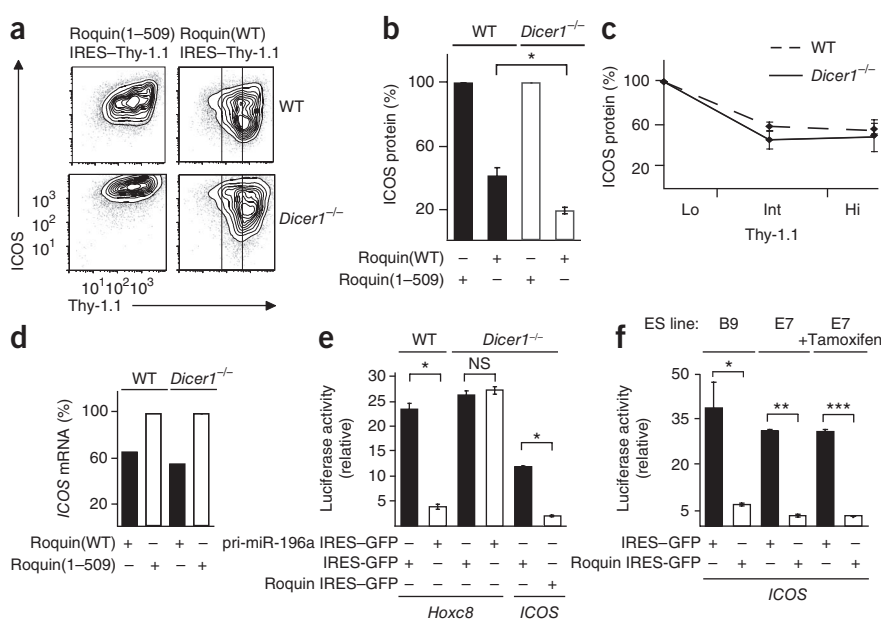
**Figure 4** Roquin protein is associated with Rck and Edc4 and shows functional dependence on Rck expression. **(a,b)** Immunoprecipitation (IP) of protein extracts from cultured  $T_H1$  cells **(a)** or MEFs **(b)** with magnetic beads coupled to monoclonal anti-roquin or to an irrelevant antibody (mouse immunoglobulin G (mIgG)); **a**) or isotype-matched control antibody **(b)**, followed by immunoblot analysis with antibodies (left margin) of immunoprecipitates (right) or extracts without immunoprecipitation (left). **(c)** Immunoprecipitation of protein extracts, with polyclonal anti-GFP, from MEFs overexpressing (overexpr) a GFP-tagged deletion mutant of roquin (roquin(1–509)) or GFP alone (above lanes), with (right) or without (left) RNase treatment. EtBr (bottom) ethidium bromide–stained agarose gel loaded with RNA extracts of supernatants from immunoprecipitates, to control for RNase treatment. **(d)** Immunoblot analysis of Rck expression in MEFs transduced with retrovirus encoding ICOS and roquin and superinfected with adenovirus encoding empty vector control, scrambled (scr) or *Rck*-specific shRNA. **(e)** Expression of ICOS and roquin (assessed as Thy-1.1) in cells transduced with roquin (middle and right) or without roquin (left) and superinfected with adenovirus encoding control or *Rck*-specific shRNA. **(f)** ICOS expression in the cells in **e**, presented relative to ICOS expression in control cells, set as 100%. \* $P = 0.034$  (one-way ANOVA). Data are representative of three independent experiments (average and s.d. in **f**).



We also did functional tests of Dicer-deficient cells and measured miR-196a-induced repression of the *Hoxc8* 3' UTR, a well-established target of this miRNA<sup>28</sup>. We found that the *Hoxc8* 3' UTR was considerably repressed by coexpression of a construct that contained the sequence of the primary transcript of miR-196a in wild-type cells but not in Dicer-deficient cells (Fig. 5e). In contrast, Dicer-deficient cells impaired in miRNA biogenesis and gene silencing were still able to support roquin-mediated repression of a luciferase reporter through the 3' UTR of *ICOS* mRNA (Fig. 5e). We next sought to determine whether roquin must act together with central components of the

RISC to induce repression of ICOS. We tested roquin-induced down-regulation of the *ICOS* 3' UTR in embryonic stem cells homozygous for deletion of genes encoding the central RISC components Ago1, Ago3 and Ago4 (*Eif2c1*, *Eif2c2* and *Eif2c3*, respectively (called 'Ago1', 'Ago3' and 'Ago4' here); line B9)<sup>29</sup>. We also analyzed the embryonic stem cell line E7 that is deficient in endogenous mouse Ago1–Ago4 but can still be expanded in culture because of low expression of a human transgene encoding Ago2 from a *loxP*-flanked locus. In these cells, the human transgene can be ablated by means of estrogen receptor–fused Cre recombinase induced by treatment with tamoxifen.

**Figure 5** Roquin-mediated ICOS repression does not depend on miRNAs or miRISC formation. **(a–d)** Expression of ICOS and roquin (assessed as Thy-1.1; **a**) and expression of ICOS protein **(b,c)** and *ICOS* mRNA **(d)** in *Dicer1*<sup>−/−</sup> and wild-type MEFs transduced with retroviruses to coexpress ICOS and roquin proteins. In **c**, ICOS expression in cells with intermediate (Int) or high (Hi) surface expression of Thy-1.1 is compared with that of low (Lo) surface expression of Thy-1.1, set as 100%. In **b,d**, ICOS expression is compared with that of cells expressing roquin(1–509), set as 100%. \* $P = 0.046$  (**b**; one-way ANOVA). Data are from one experiment (**a,d**) or three independent experiments (**b,c**; average and s.d.). **(e)** Luciferase activity in wild-type and *Dicer1*<sup>−/−</sup> MEFs coinfecting with the dual-luciferase reporter (with *Hoxc8* 3' UTR or *ICOS* 3' UTR cloned behind renilla luciferase) and adenoviruses (left margin), presented as the ratio of renilla luciferase units to firefly luciferase units. pri-miR-196a, primary transcript of miR-196a. \* $P < 0.0001$ ; NS,  $P = 0.217$  (one-way ANOVA). **(f)** Luciferase activity in the embryonic stem cell lines B9 and E7 coinfecting as in **e** and left untreated (left and middle) or treated with tamoxifen (right). \* $P = 0.003$ , \*\* $P < 0.0001$  and \*\*\* $P < 0.0001$  (one-way ANOVA). Data are from three independent experiments (average and s.d.).



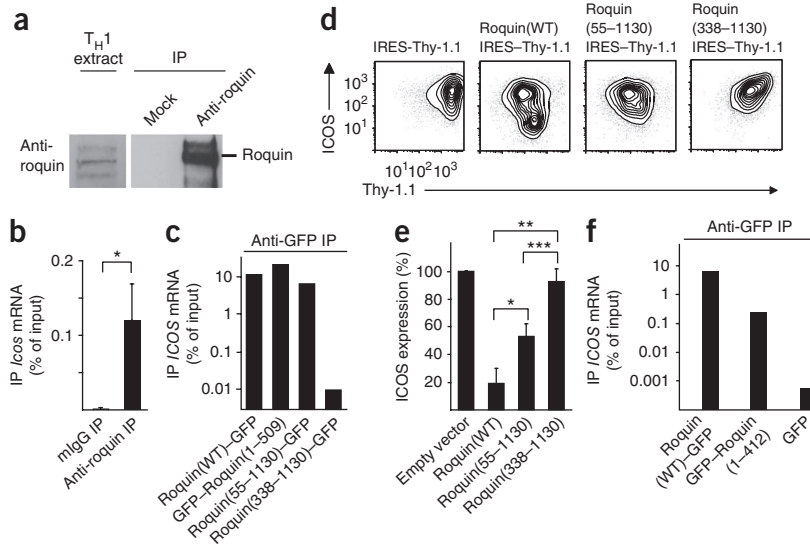


**Figure 6** Roquin binds to *ICOS* mRNA through its ROQ and zinc-finger domains. **(a)** Immunoblot analysis of roquin in  $T_H1$  cell extracts before (left) and after (right) immunoprecipitation with polyclonal anti-roquin beads or precipitation with empty beads (Mock). Data are representative of three experiments. **(b)** RT-PCR analysis of endogenous *ICOS* mRNA in the precipitates in **a**, presented as percentage of input. \* $P = 0.012$  (one-way ANOVA). Data are representative of three independent experiments (average and s.d.). **(c)** RT-PCR analysis of *ICOS* mRNA in anti-GFP immunoprecipitates from extracts of HEK293 cells transfected with *ICOS* (full-length) and GFP-tagged wild-type or deletion mutants of roquin, presented as the percentage of *ICOS* mRNA in RNA extracts from input samples. Data are representative of two experiments. **(d,e)** Expression of *ICOS* and roquin (assessed as Thy-1.1; **d**) and *ICOS* expression (**e**) in MEFs sequentially transduced with retrovirus encoding *ICOS* and wild-type or mutant roquin. \* $P = 0.002$ ; \*\* $P = 0.001$ ; \*\*\* $P = 0.006$  (one-way ANOVA). Data are from one experiment representative of three (**d**) or are from three independent experiments (**e**; average and s.d.). **(f)** Coimmunoprecipitation of RNA as in **c**. Data are representative of two experiments.

After tamoxifen treatment, these cells remain viable for up to 4 d before undergoing apoptosis<sup>29</sup>. Adenoviral coinfection of the *ICOS* 3' UTR reporter construct with GFP or with GFP coexpressed from an internal ribosomal entry site with roquin (**Fig. 5f**) showed that roquin was able to repress the *ICOS* 3' UTR in cells lacking mouse Ago1, Ago3 and Ago4 (line B9) and in cells lacking mouse Ago1–Ago4 but containing small amounts of human Ago2 (line E7). After treatment with tamoxifen, E7 cells were arrested in proliferation but were not impaired in roquin-mediated repression of *ICOS*, as determined by measurement of luciferase activity (**Fig. 5f**) and flow cytometry (data not shown). The ratio of renilla luciferase activity to firefly luciferase activity provides a measurement of *ICOS* 3' UTR-mediated repression of renilla luciferase expression. This is independent of infection efficiency, epigenetic regulation of the adenoviral episomes and the relative transcription or translation efficiencies of various cell types. Comparing these normalized values, we did not find evidence that repression of the *ICOS* 3' UTR changed after partial or complete inactivation of miRISC function. Therefore, we did not detect regulation of the *ICOS* 3' UTR via miRNAs in embryonic stem cells (**Fig. 5f**). However, we cannot exclude the possibility of miRNA-dependent regulation of *ICOS* in other cell types. In fact, we measured *ICOS* mRNA expression from retroviruses that integrated into the genome of Dicer-deficient and wild-type MEFs, normalized to that of *Hprt1* (encoding hypoxanthine guanine phosphoribosyl transferase; **Supplementary Fig. 3g**), and compared that expression with the amount of quantitative genomic PCR amplification of the retroviral vector-encoded GFP sequence normalized to that of *Hist1h2ak* (encoding histone cluster 1, H2ak; **Supplementary Fig. 3h**). We found slightly more *ICOS* expression per integration in Dicer-deficient cells (**Supplementary Fig. 3i**), which suggested a moderate

repressive effect of miRNAs on the *ICOS* 3' UTR in MEFs. Together these findings cannot exclude the possibility of cell type-specific regulation of *ICOS* by miRNAs but rule out a requirement for miRNAs and RISC formation in roquin-mediated *ICOS* repression.

### Roquin is an RNA-binding protein

We next assessed whether roquin itself interacts with mRNA. First we addressed whether we could detect endogenous mouse *Icos* mRNA in endogenous roquin immunoprecipitates from protein extracts of primary  $T_H1$  cells. We documented efficient roquin protein enrichment in immunoprecipitates (**Fig. 6a**) and confirmed physical association of *Icos* mRNA and roquin protein by showing significantly more PCR amplification of *Icos* in the roquin immunoprecipitation than in mock precipitations (**Fig. 6b**). The observed interaction did not depend on the carboxyl terminus of roquin but depended on its amino terminus. In fact, the interaction of roquin and *ICOS* mRNA after cotransfection in HEK293 cells was the same or slightly greater for the roquin(1–509) mutant (**Fig. 6c**). Deletion of the amino-terminal RING finger alone in roquin(55–1130) had a small negative effect on the interaction with *ICOS* mRNA (**Fig. 6c**). However, binding to *ICOS* mRNA was lost when the amino-terminal deletion in the roquin(338–1130) mutant included the ROQ domain (**Fig. 6c**). Roquin-mediated repression of *ICOS* was completely abolished when the RING finger and ROQ domain were deleted in roquin(338–1130), whereas deletion of the RING finger alone in roquin(55–1130) had a partial effect (**Fig. 6d,e**). To address a possible contribution of the CCCH-type zinc finger, we expressed the truncated roquin protein roquin(1–412), which contained the RING finger and ROQ domain but lacked the carboxy-terminal sequences, including the zinc finger. This mutant showed considerable impairment in binding to *ICOS* mRNA; however, it associated with more *ICOS* mRNA than control immunoprecipitates (**Fig. 6f**). These findings show that the zinc finger acts together with the ROQ domain, which is critical in the binding to *ICOS* mRNA.

Finally, we investigated whether roquin, in the absence of other cellular factors, was able to bind and recognize *ICOS* mRNA. We bacterially expressed and purified an amino-terminal fragment of roquin(1–441), which contained the RING finger, ROQ and zinc finger domains (**Supplementary Fig. 4a**). We incubated the protein with capped full-length *ICOS* mRNA generated by *in vitro* transcription with T7 polymerase (**Supplementary Fig. 4b**). In electrophoretic mobility-shift assays, roquin protein interacted with full-length *ICOS* mRNA (**Fig. 7a**), and the roquin-induced retardation of the *ICOS* mRNA band was greater with higher concentrations of roquin in the binding reaction (**Fig. 7a**). The progressive upshift increased over a wide range of protein concentrations (**Fig. 7a**), which indicated the existence of several binding sites for roquin on *ICOS* mRNA.

Expression of *ICOS* mRNA from a construct lacking the 3' UTR is not repressed in cells overexpressing roquin<sup>1</sup>. Consistent with that finding, we did not detect any regulation of *ICOS* mRNA by

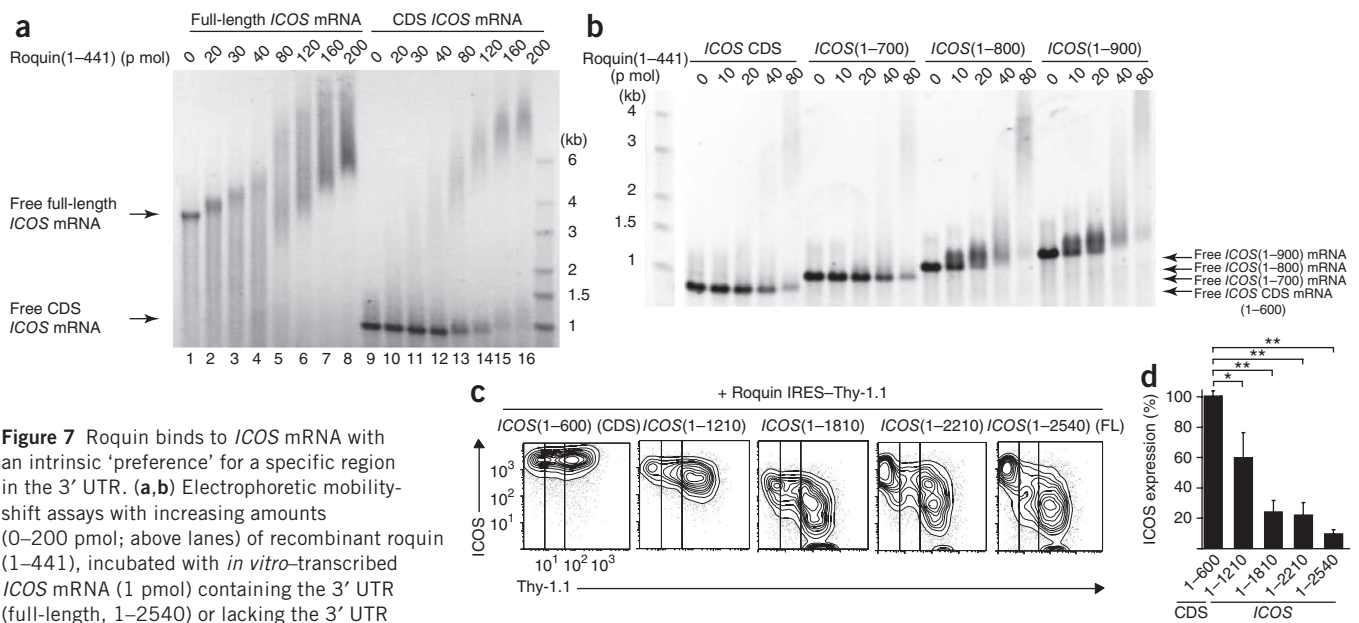


**Figure 7** Roquin binds to *ICOS* mRNA with an intrinsic 'preference' for a specific region in the 3' UTR. (**a,b**) Electrophoretic mobility-shift assays with increasing amounts (0–200 pmol; above lanes) of recombinant roquin (1–441), incubated with *in vitro*-transcribed *ICOS* mRNA (1 pmol) containing the 3' UTR (full-length, 1–2540) or lacking the 3' UTR (coding sequence (CDS), 1–600; **a**) or with *ICOS* mRNA in which the 3' UTR was progressively shortened from 900 bases (*ICOS*(1–900)) to 700 bases (*ICOS*(1–700)); **b**). (**c,d**) Expression of *ICOS* and roquin (assessed as Thy-1.1; **c**) and *ICOS* (**d**) in MEFs sequentially transduced with retrovirus encoding roquin and *ICOS* or *ICOS* mRNA with a progressively shortened 3' UTR. In **d**, *ICOS* expression in cells with high Thy-1.1 expression is presented relative to its expression in Thy-1.1-negative cells. FL, full-length. \* $P = 0.015$  and \*\* $P < 0.001$  (one-way ANOVA). Data are from one experiment representative of three (**c**) or are from three independent experiments (**d**; average and s.d.).

roquin when we replaced the 3' UTR of *ICOS* with an unrelated 3' UTR (data not shown) or with a nonresponsive sequence (that is, a second coding sequence of *ICOS* without start and stop codons; **Supplementary Fig. 5a**, bottom). Only full-length *ICOS* containing the 3' UTR was efficiently bound by roquin *in vitro*, whereas the *ICOS* coding sequence (**Fig. 7a**) or tandem coding sequences of *ICOS* (**Supplementary Fig. 5b**) were not well recognized and their mobility was not altered by roquin at low concentrations (**Supplementary Fig. 5b**). Furthermore, roquin did not alter the mobility of excess yeast transfer RNA included in the binding reaction (**Supplementary Fig. 4c**), and under these conditions, an unrelated protein did not induce retardation of the full-length *ICOS* mRNA band (**Supplementary Fig. 4d**). The binding was not due to the T7 terminator sequence (**Supplementary Fig. 4e,f**) and was not dependent on the attachment of a poly(A) tail (data not shown). However, at high protein concentrations, the mobility of the coding sequence was also altered by roquin protein. We therefore quantified the effective roquin protein concentration required for complete binding of various constructs, as determined by the disappearance of free mRNA. Full upshift of free full-length *ICOS* mRNA became apparent at concentrations as low as 20 pmol, whereas complete upshift of *ICOS* coding sequence mRNA did not occur at concentrations below 160 pmol roquin per binding reaction (**Fig. 7a**), which indicated a difference of approximately eightfold in the affinity of roquin for the two different mRNAs. We mapped the site in the 3' UTR of *ICOS* required for the binding of higher affinity by introducing progressive deletions of 600 base pairs starting from the 3' end. An *ICOS* 3' UTR mRNA construct of residues 1–1210, containing the coding sequence and the first 610 base pairs of the 3' UTR, had a response to roquin binding indistinguishable from that of full-length *ICOS* (**Supplementary Fig. 6a**). Roquin(1–441) bound this minimal *ICOS* 3' UTR construct (1–1210) with higher affinity than did an irrelevant mRNA of similar length (the coding sequence of human *FOXP3* (encoding the transcription factor Foxp3); **Supplementary Fig. 6b**). By removing in a stepwise

manner 100 base pairs from the 3' end of this *ICOS* construct (**Fig. 7b**), we identified the region between 100 and 200 base pairs 3' of the stop codon as being critical for the higher affinity binding of roquin to the *ICOS* 3' UTR. We also correlated the sequences required for the higher affinity binding of *ICOS* mRNA by roquin with the extent of functional repression of *ICOS* by roquin in MEFs (**Fig. 7c,d**). All constructs containing the mapped binding site were repressed by roquin. However, the degree of *ICOS* repression by roquin increased with length of the *ICOS* 3' UTR. These findings indicate that multiple sites in the 3' UTR may actually contribute to the functional repression of *ICOS* by roquin in living cells.

## DISCUSSION

Our data have indicated the involvement of P-body components in roquin-mediated repression of *ICOS*. We have shown that localization of roquin to P bodies occurred in primary CD4<sup>+</sup> T cells as well as in HEK293 cells and was detected equally by colocalization with Rck or Edc4, two different P-body markers. In fact, in HEK293 or CD4<sup>+</sup> T cells not subjected to stress, we did not find colocalization of roquin-enriched foci with the stress granule markers FMRP or G3BP1. The localization to P bodies required the carboxyl terminus of roquin, which contains sequences enriched for glutamine and asparagine. Glutamine stretches have been shown to act as polar zippers in prion proteins<sup>24</sup>, and more glutamine and asparagine residues have also been found in many P-body proteins. These regions are believed to permit protein-protein interactions important for the formation of messenger ribonucleoproteins in post-transcriptional regulation<sup>23,25</sup>. The presence and the functional importance of sequences enriched for glutamine and asparagine provide support for the idea of an evolutionary conserved role for roquin in the P-body pathway. In the context of the reported localization of roquin to stress granules<sup>2,30</sup>, we noted that roquin translocated into stress granules after induction of stress in HEK293 and CD4<sup>+</sup> T cells and it is therefore possible that cells undergoing a stress response have

altered roquin activity. So far, we have not been able to obtain experimental support for this idea. We have shown that roquin effectively repressed ICOS in helper T cells in a phase in which the TIA-1-dependent integrated stress response has been shown to repress translation of *IL4* mRNA (encoding interleukin 4)<sup>31</sup>. However, we did not observe any effect on roquin activity in MEFs deficient in TIA-1. In the P-body pathway, we identified binding of roquin to the P-body components Edc4 and Rck in CD4<sup>+</sup> T cells and MEFs and demonstrated the importance of Rck expression for roquin function. Rck and Edc4 operate in the decapping pathway and destabilize mRNAs in functional cooperation with Dcp1a and Dcp2, the latter of which removes the 5' N7-methylguanosine cap. The mRNAs that lack this modification are no longer protected from 5'-to-3' mRNA degradation<sup>23</sup>. Nevertheless, the repression of mRNA translation by interference with binding of the translation-initiation factor complex eIF4F to the 5' N7-methylguanosine cap of the mRNA represents the rate-limiting step of decapping<sup>32–34</sup>. Therefore, although they do not exclude the possibility of a role for roquin in the first step of translational repression, our results suggest that roquin promotes decapping of target mRNAs.

We have also presented evidence that roquin is an RNA-binding protein. The observed association of roquin and ICOS mRNA in T cell extracts or cell extracts from transfected HEK293 cells depended mainly on the ROQ domain, which shows that this domain is a member of a relatively small group of RNA-binding modules<sup>35</sup>. It seems that the ROQ domain binds in combination with the CCCH-type zinc finger module in roquin. This mode of protein-RNA interaction allowed binding of multiple roquin molecules to the same ICOS mRNA *in vitro*. The cooperation of different RNA-binding modules in one protein has been described as a common feature of RNA-binding proteins and typically enables them to bind with higher affinity or to obtain specificity for an mRNA substrate among an enormous diversity of possible structures<sup>35</sup>. These findings are consistent with a report also demonstrating that the ROQ domain is critical for the binding of roquin to a short RNA fragment from the ICOS 3' UTR<sup>30</sup>. However, we found that roquin had a 'preference' for certain structure or sequence determinants present in a previously unrecognized region of the ICOS mRNA, which probably specify the cellular targets of roquin. Our experiments showed roquin bound with higher affinity to a specific sequence located between 100 and 200 base pairs downstream of the stop codon in the ICOS 3' UTR. In addition, we found general binding to various other mRNAs with lower affinity, which indicates the possibility that sequential binding on the ICOS mRNA could occur in a cooperative manner. We conclude that roquin is a protein that has a low affinity for mRNAs in general. However, roquin has also a protein-intrinsic higher affinity for sequence or structure determinants of the ICOS 3' UTR. The fact that the ICOS 3' UTR contributes more regulatory elements than just one single roquin-specific binding site for efficient repression of ICOS in cells indicates the involvement of additional steps beyond binding. Therefore, we propose that the repression occurs in a higher order structure induced by recognition of the ICOS 3' UTR by roquin but at the same time needs cellular cofactors that may require additional features in the ICOS 3' UTR.

We analyzed roquin activity in cells deficient in Dicer and Ago1–Ago4. We did not find evidence for a positive role of the miRISC, as suggested by studies describing that silencing of ICOS by roquin requires an intact miR-101-recognition motif<sup>1</sup>. In those experiments, a critical region in the 3' UTR of ICOS was mapped and a minimal response element of 47 base pairs was defined<sup>1</sup>. We assume that experimental differences related to the use of isolated fragments linked to

reporters or, in our case, the entire 3' UTR in the context of the ICOS coding sequence may account for the contrasting conclusions.

The newly described molecular functions of roquin may be involved in the prevention of autoimmunity. These functions include sequence- or structure-specific binding to RNA as well as the formation of complexes with other factors involved in mRNA decay. We speculate that at least one of these functions could be impaired in roquin proteins with the methionine-to-arginine substitution at position 199 in the ROQ domain and could thereby cause the development of autoimmune disease in *Rc3h1<sup>san/san</sup>* mice<sup>2</sup>.

## METHODS

Methods and any associated references are available in the online version of the paper at <http://www.nature.com/natureimmunology/>.

*Note: Supplementary information is available on the Nature Immunology website.*

## ACKNOWLEDGMENTS

We thank M. Schmidt-Suppran and D. Niessing for critical reading of the manuscript and discussions; G. Stoecklin for unpublished observations and advice; C. Vinuesa (The John Curtin School of Medical Research, Canberra, Australia) for ICOS and roquin cDNA; G. Hannon (Cold Spring Harbor Laboratory) for *Dicer1<sup>fl/+</sup>* mice; C. Wilson (University of Washington) for Tg(Cd4-cre) mice; N. Kedersha and P. Anderson (Brigham and Women's Hospital) for TIA-1-knockout MEFs; U. Fischer (Biozentrum Würzburg) for anti-FMRP; H. Sarioglu for mass-spectrometry analysis; and C. Thirion and L. Behrend (Sirion Biotech) for advice and reagents for adenoviral infection. Supported by Deutsche Forschungsgemeinschaft (SFB 571 to V.H.) and Fritz Thyssen Foundation (V.H.).

## AUTHOR CONTRIBUTIONS

E.G. did most experiments, with the help of K.P.H., N.R. and C.W.; K.U.V. contributed to some experiments and edited the manuscript; L.D., E.K. and X.W. established tools and provided advice; E.G. and V.H. planned the project together; and V.H. supervised the experiments and wrote the manuscript.

## COMPETING FINANCIAL INTERESTS

The authors declare no competing financial interests.

Published online at <http://www.nature.com/natureimmunology/>.

Reprints and permissions information is available online at <http://npg.nature.com/reprintsandpermissions/>.

1. Yu, D. *et al.* Roquin represses autoimmunity by limiting inducible T-cell co-stimulator messenger RNA. *Nature* **450**, 299–303 (2007).
2. Vinuesa, C.G. *et al.* A RING-type ubiquitin ligase family member required to repress follicular helper T cells and autoimmunity. *Nature* **435**, 452–458 (2005).
3. Anderson, P., Phillips, K., Stoecklin, G. & Kedersha, N. Post-transcriptional regulation of proinflammatory proteins. *J. Leukoc. Biol.* **76**, 42–47 (2004).
4. Hao, S. & Baltimore, D. The stability of mRNA influences the temporal order of the induction of genes encoding inflammatory molecules. *Nat. Immunol.* **10**, 281–288 (2009).
5. Hoefig, K.P. & Heissmeyer, V. MicroRNAs grow up in the immune system. *Curr. Opin. Immunol.* **20**, 281–287 (2008).
6. Stefl, R., Skrisovska, L. & Allain, F.H. RNA sequence- and shape-dependent recognition by proteins in the ribonucleoprotein particle. *EMBO Rep.* **6**, 33–38 (2005).
7. Jing, Q. *et al.* Involvement of microRNA in AU-rich element-mediated mRNA instability. *Cell* **120**, 623–634 (2005).
8. Kedde, M. *et al.* RNA-binding protein Dnd1 inhibits microRNA access to target mRNA. *Cell* **131**, 1273–1286 (2007).
9. Vasudevan, S. & Steitz, J.A. AU-rich-element-mediated upregulation of translation by FXR1 and Argonaute 2. *Cell* **128**, 1105–1118 (2007).
10. Tan, A.H., Wong, S.C. & Lam, K.P. Regulation of mouse inducible costimulator (ICOS) expression by Fyn-NFATc2 and ERK signaling in T cells. *J. Biol. Chem.* **281**, 28666–28678 (2006).
11. Bossaller, L. *et al.* ICOS deficiency is associated with a severe reduction of CXCR5+CD4 germinal center Th cells. *J. Immunol.* **177**, 4927–4932 (2006).
12. Dong, C. *et al.* ICOS co-stimulatory receptor is essential for T-cell activation and function. *Nature* **409**, 97–101 (2001).
13. Dong, C., Temann, U.A. & Flavell, R.A. Cutting edge: critical role of inducible costimulator in germinal center reactions. *J. Immunol.* **166**, 3659–3662 (2001).

14. McAdam, A.J. *et al.* Mouse inducible costimulatory molecule (ICOS) expression is enhanced by CD28 costimulation and regulates differentiation of CD4<sup>+</sup> T cells. *J. Immunol.* **165**, 5035–5040 (2000).
15. Tafuri, A. *et al.* ICOS is essential for effective T-helper-cell responses. *Nature* **409**, 105–109 (2001).
16. Linterman, M.A. *et al.* Follicular helper T cells are required for systemic autoimmunity. *J. Exp. Med.* **206**, 561–576 (2009).
17. Wan, Y.Y. *et al.* Transgenic expression of the coxsackie/adenovirus receptor enables adenoviral-mediated gene delivery in naive T cells. *Proc. Natl. Acad. Sci. USA* **97**, 13784–13789 (2000).
18. Oberdoerffer, P. *et al.* Efficiency of RNA interference in the mouse hematopoietic system varies between cell types and developmental stages. *Mol. Cell. Biol.* **25**, 3896–3905 (2005).
19. Heissmeyer, V., Ansel, K.M. & Rao, A. A plague of autoantibodies. *Nat. Immunol.* **6**, 642–644 (2005).
20. Chu, C.Y. & Rana, T.M. Translation repression in human cells by microRNA-induced gene silencing requires RCK/p54. *PLoS Biol.* **4**, e210 (2006).
21. Didiot, M.C., Subramanian, M., Flatter, E., Mandel, J.L. & Moine, H. Cells lacking the fragile X mental retardation protein (FMRP) have normal RISC activity but exhibit altered stress granule assembly. *Mol. Biol. Cell* **20**, 428–437 (2009).
22. Mazroui, R. *et al.* Trapping of messenger RNA by fragile X mental retardation protein into cytoplasmic granules induces translation repression. *Hum. Mol. Genet.* **11**, 3007–3017 (2002).
23. Franks, T.M. & Lykke-Andersen, J. The control of mRNA decapping and P-body formation. *Mol. Cell* **32**, 605–615 (2008).
24. Michelitsch, M.D. & Weissman, J.S. A census of glutamine/asparagine-rich regions: implications for their conserved function and the prediction of novel prions. *Proc. Natl. Acad. Sci. USA* **97**, 11910–11915 (2000).
25. Reijns, M.A., Alexander, R.D., Spiller, M.P. & Beggs, J.D. A role for Q/N-rich aggregation-prone regions in P-body localization. *J. Cell Sci.* **121**, 2463–2472 (2008).
26. Gilks, N. *et al.* Stress granule assembly is mediated by prion-like aggregation of TIA-1. *Mol. Biol. Cell* **15**, 5383–5398 (2004).
27. Parameswaran, P. *et al.* Six RNA viruses and forty-one hosts: viral small RNAs and modulation of small RNA repertoires in vertebrate and invertebrate systems. *PLoS Pathog.* **6**, e1000764 (2010).
28. Yekta, S., Tabin, C.J. & Bartel, D.P. MicroRNAs in the Hox network: an apparent link to posterior prevalence. *Nat. Rev. Genet.* **9**, 789–796 (2008).
29. Su, H., Trombly, M.I., Chen, J. & Wang, X. Essential and overlapping functions for mammalian Argonautes in microRNA silencing. *Genes Dev.* **23**, 304–317 (2009).
30. Athanasopoulos, V. *et al.* The ROQUIN family of proteins localizes to stress granules via the ROQ domain and binds target mRNAs. *FEBS J.* **277**, 2109–2127 (2010).
31. Scheu, S. *et al.* Activation of the integrated stress response during T helper cell differentiation. *Nat. Immunol.* **7**, 644–651 (2006).
32. Cougot, N., van Dijk, E., Babajko, S. & Seraphin, B. 'Cap-tabolism'. *Trends Biochem. Sci.* **29**, 436–444 (2004).
33. Eulalio, A., Behm-Ansmant, I. & Izaurralde, E. P bodies: at the crossroads of post-transcriptional pathways. *Nat. Rev. Mol. Cell Biol.* **8**, 9–22 (2007).
34. Parker, R. & Sheth, U. P bodies and the control of mRNA translation and degradation. *Mol. Cell* **25**, 635–646 (2007).
35. Lunde, B.M., Moore, C. & Varani, G. RNA-binding proteins: modular design for efficient function. *Nat. Rev. Mol. Cell Biol.* **8**, 479–490 (2007).

## ONLINE METHODS

**Mice.** Mice (from Taconic Farms) were housed in a specific pathogen-free barrier facility and were used at 6–12 weeks of age in accordance with the Helmholtz Zentrum München institutional, state and federal guidelines.

**Cell culture and transfection.** HEK293 cells and MEFs were grown in DMEM with 10% (vol/vol) FCS, penicillin-streptomycin (1,000 U/ml) and HEPES (10 mM), pH 7.4. Embryonic stem cells were grown first on feeder cells in DMEM containing 20% (vol/vol) FCS, L-glutamine (2 mM), penicillin-streptomycin (100 U/ml), sodium pyruvate (1 mM), nonessential amino acids (0.1 mM),  $\beta$ -mercaptoethanol (0.1 mM) and leukemia-inhibitory factor (2,000 U/ml) and were passaged twice on 0.1% (wt/vol) gelatin. Peripheral CD4<sup>+</sup> T cells were isolated with CD4 Dynabeads (Invitrogen), were kept in RPMI medium (with 10% (vol/vol) FCS,  $\beta$ -mercaptoethanol (0.1 mM), penicillin-streptomycin (100 U/ml) and HEPES (10 mM), pH 7.2) and were stimulated for 36–48 h under T<sub>H</sub>0 conditions (on surfaces coated with goat anti-hamster immunoglobulin G (55397; MP Biomedicals) plus anti-CD3 (0.1  $\mu$ g/ml; 145-2C11) and anti-CD28 (1  $\mu$ g/ml; 37N); both purified in-house); T<sub>H</sub>1 conditions (inclusion of antibody to interleukin 4 (anti-IL-4; 10  $\mu$ g/ml; IIB11; purified in-house) and recombinant IL-12 (10 ng/ml; R&D Systems); or T<sub>H</sub>2 conditions (inclusion of anti-IL-12 (3  $\mu$ g/ml; C17.8) and anti-interferon- $\gamma$  (5  $\mu$ g/ml; Xmg1.2); both purified in-house, as well as supernatants of I3L6 mouse myeloma cells containing mouse IL-4 (which corresponds to 1,000 U/ml of recombinant IL-4)). Tosyl-activated M-450 beads (Invitrogen) coupled to anti-CD28 and anti-CD3 were used for bead stimulation. After being stimulated for 48 h, cell populations were expanded in recombinant human IL-2 (10 U/ml; World Health Organization, National Institute for Biological Standards and Control). All monoclonal antibodies were purified from supernatants of hybridomas on protein A Sepharose columns (145-2C11 and 37N) or protein G Sepharose columns (Xmg1.2, IIB11, C17.8 and anti-Roq hybridomas) and were dialyzed against PBS.

**Virus production.** Type 5 replication-deficient adenovirus was produced by transfection of adenoviral vectors into HEK293 cells, followed by purification according to the manufacturer's instructions (Cell Biolabs). Retroviral supernatants were produced by calcium-phosphate transfection of HEK293T cells with amphotropic packaging vectors and retroviral expression vectors. Supernatants were collected 72 h after transfection, were filtered through 0.45- $\mu$ m filters and were used for spin-infection. Transduced cells were analyzed 3–4 d after infection on a FACSCalibur or were sorted on a FACSAria II (Becton Dickinson).

**Adenoviral knockdown or ectopic protein expression.** Adenoviral vectors (Sirion Biotech) with control shRNA (5'-TTTTTGGCCTTTTGTAGCTG-3'), scrambled shRNA (5'-ACAAGATGAAGAGCACCAA-3'), *Rc3h1*-specific shRNA (5'-CGCACAGTTACAGAGCTCATT-3'), *Cd4*-specific shRNA (5'-CACAGCTATCACGGCCTATAA-3') or *Rck*-specific shRNA (5'-GCCAAGAATATGTCTTTATA-3') were placed under the control of a polymerase III-dependent small nuclear RNA U6 promoter and were coexpressed with phosphoglycerate kinase promoter-driven GFP. The adenoviral expression vector was created by assembly of the artificial CAG promoter in front of a Gateway cassette followed by a poly(A) signal from bovine growth hormone in the pAd-Pl vector (Invitrogen), into which GFP-tagged roquin was inserted by means of lambda recombination from the pENTR 11 vector (Invitrogen).

**Luciferase assay.** MEFs plated on 12-well plates were infected with adenovirus. After 2 d, a dual-luciferase reporter assay (Promega) was done. Cells were lysed in 150  $\mu$ l lysis buffer, lysates were cleared by centrifugation and 20  $\mu$ l supernatant was analyzed.

**Real-time PCR.** RNA was isolated from cells or immunoprecipitates with TRIzol (Sigma) or a MirVana kit (Ambion), respectively. After reverse transcription with the Quantitect kit (Qiagen), quantitative PCR assays were done (primers and universal probes, **Supplementary Table 1**; Roche). Expression of

miRNA was measured by quantitative PCR and normalized to that of the small nuclear RNA U6 after the use of TaqMan microRNA Reverse Transcription kit and stem-loop primers specific for miR-101, miR-328, miR-196a miR-214, miR-155, miR-181 and U6 (Applied Biosystems). A LightCycler 480II and Light Cycler 480 software release 1.5.0 SP1 were used for quantitative PCR.

**Confocal microscopy.** HEK293 cells were transfected with FuGENE reagent (Roche), then were seeded on glass cover slips and subjected to stress for 1 h at 37 °C with 0.5 mM sodium arsenite (Sigma). Diagnostica glass cover slips were coated first with 0.01% (wt/vol) poly-L-lysine and then with anti-CD3 (2.5  $\mu$ g/ml) and anti-CD28 (5  $\mu$ g/ml) before the addition of T cells in a volume of 50  $\mu$ l. Cells were fixed with 4% (wt/vol) paraformaldehyde and were washed three times in 0.5% (vol/vol) Nonidet-P40, 0.01% (wt/vol) NaN<sub>3</sub> and 10% (vol/vol) FCS in PBS. Antibody to p70 S6 kinase- $\alpha$  (sc-8418; Santa Cruz), anti-G3BP (sc-81940; Santa Cruz) and anti-Rck (A300-461A; Bethyl) or anti-FMRP (a gift from U. Fischer) was used for staining in combination with secondary antibodies coupled to indocarbocyanine (111-176-144; Jackson Laboratories) or indocarbocyanine (715-165-151; Jackson Laboratories). Images were captured on a Leica DM IRBE microscope and were analyzed with LCS Lite software.

**Coimmunoprecipitation of roquin-associated ICOS mRNA or protein.** This was done as described<sup>36</sup>. T cells ( $2 \times 10^8$ ) or HEK293 cells ( $1 \times 10^7$ ) were lysed on ice in 2 ml lysis buffer (20 mM Tris, pH 7.5, 150 mM NaCl, 0.25% (vol/vol) Nonidet-P40, 1.5 mM MgCl<sub>2</sub>, protease inhibitor mix without EDTA (Roche) and 1 mM dithiothreitol). Lysates were passaged through a 26-gauge needle, then were shock frozen and thawed and then cleared by centrifugation. Anti-roquin (A300-514A; Bethyl) or anti-GFP (A11122; Invitrogen) bound to protein G magnetic beads (Invitrogen) was incubated for 4 h at 4 °C with lysates in the presence of 20 U RNasin. Beads were washed two times (RNA) or three times (protein) with lysis buffer with the inclusion of two additional washes (RNA) with lysis buffer containing 300 mM NaCl, 0.5% (vol/vol) Nonidet-P40 and 2.5 mM MgCl<sub>2</sub>.

**Purification of roquin protein.** Roquin(1–441) was expressed from the petM11 bacterial expression vector (modified; Novagen) in bacteria, was purified by histidine-tag chromatography (GE Healthcare) and was desalted via PD10 gel filtration (GE Healthcare).

**In vitro RNA transcription.** For *in vitro* transcription, inserts containing the mRNA and 3' UTR in the bacterial expression vector pDest17 (Invitrogen) were linearized by digestion with restriction enzymes. The mMessage mMachine T7 transcription kit was used according to the manufacturers' instructions (Ambion) for *in vitro* transcription of mRNA, and RNA was purified with an RNeasy Kit (Qiagen).

**Mass spectrometry.** For the identification of coimmunoprecipitated proteins, slices of SDS-polyacrylamide gels were analyzed by a liquid chromatography-tandem mass spectrometry approach with an LTQ Orbitrap XL mass spectrometer coupled to an Ultimate 3000 Nano-HPLC. All tandem mass spectrometry spectra were then analyzed with the Mascot search engine against the UniProt reference cluster (uniref100\_mouse fasta) protein database. Protein identifications were accepted if they could be established at a probability of greater than 95% and contained at least two identified peptides.

**Electrophoretic mobility-shift assay.** Samples were separated by electrophoresis through native 0.75% agarose gels, then were stained with ethidium bromide. Recombinant protein (5–160 pmol) was incubated for 20 min on ice with ICOS mRNA (0.6 or 1 pmol) in a solution of 150 mM KCl, 50 mM Tris-HCl, pH 7.4, 1 mM MgCl<sub>2</sub>, 1 mM EDTA and 1 mM dithiothreitol, and then was adjusted to a concentration of 16% (vol/vol) glycerol.

36. Weinmann, L. *et al.* Importin 8 is a gene silencing factor that targets argonaute proteins to distinct mRNAs. *Cell* **136**, 496–507 (2009).